CHEMISTRY
A EUROPEAN JOURNAL

DOI: 10.1002/chem.200902459

Shifting Paradigms: Electrostatic Interactions and Covalent Bonding

Heiko Jacobsen*[a]

Abstract: The role of electrostatic interactions in covalent bonding of heavier main group elements has been evaluated for the exemplary set of molecules X_2H_2 (X = C, Si, Ge, Sn, Pb). Density functional calculations at PBE/QZ4P combined with energy decomposition procedures and kinetic energy density analyses have been carried out for a variety of different structures, and two factors are responsible for the fact that the heavier homologues of acetylene exhibit doubly hydrogen-bridged local minimum geometries. For one, the extended electronic core with at least one set of p orbitals of the Group 14 elements beyond the first long period is responsible for favorable electrostatic E–H interactions. This electrostatic interaction is the strongest for the isomer with two bridging hydrogen atoms. Secondly, the H substituent does not posses an electronic core or any bonding-inactive electrons, which would give rise to a significant amount of Pauli repulsion, disfavoring the doubly bridged isomer. When one of two criteria is not met the unusual doubly bridged structure no longer constitutes the energetically preferred geometry. The bonding model is validated in calculations of different structures of $Si_2(CH_3)_2$.

Keywords: bond theory · electrostatic interactions · Group 14 elements · kinetic energy density

Introduction

The transition from revolutionary science to normal science occurs when past scientific achievements that the scientific community acknowledges as supplying the foundation for its further practice advance from new discovery or novel insight to generally accepted, basic knowledge.[1] In this sense, the field of chemical bonding as the central theme for structure and reactivity is shaped by an ongoing expansion of its archetypical thought patterns. In particular, the notion of chemical bonding in main group chemistry has witnessed significant changes, and the discovery of compounds with silicon–silicon double bonds in 1981 led to a to a redefinition of the concept of bonding of main group elements beyond the first long period. In a recent review, West documented the history of this paradigm shift and outlined the events that led to the discovery of, as well as the resulting developments in multiple-bond chemistry of heavier main group elements.[2]

The synthesis and structural characterization of a silicon–silicon double bond was in sharp contrast to the general understanding of multiple bonding in inorganic chemistry,[3] and completely overturned the classical double bond rule.[4] The first investigations of a molecule containing a silicon–silicon triple bond continued to produce surprising results; its unexpected and unusual global minimum structure was yet another indication of the growing consensus that in many ways, first-row elements such as carbon are oddities and stand apart from the heavier elements in their respective groups. The common practice that models of chemical bonding, developed for elements of the first long period, are applied throughout the periodic table received more and more critical reconsideration, and the acetylene analogues of heavier Group 14 elements served as an entry into the general chemistry curriculum as to put ideas of chemical bonding into a broader perspective.[5]

As exemplified by multiple silicon–silicon bonds, the discovery of new structural motifs led to new views on chemical bonding, one of the most fundamental concepts in chemistry. However, the richness in bonding is one of the reasons why a chemical bond is not as clearly defined as one would wish, and models of chemical bonding are currently being refined and redefined not only to understand and explain unusual bonding situations, but also to develop a uni-

[a] Dr. H. Jacobsen
KemKom, 1215 Ursulines Avenue
New Orleans, LA 70116 (USA)
and
Department of Chemistry, Tulane University
New Orleans, LA 70118 (USA)
E-mail: jacobsen@kemkom.com

Supporting information for this article is available on the WWW under http://dx.doi.org/10.1002/chem.200902459.

WILEY InterScience DISCOVER SOMETHING GREAT
© 2010 Wiley-VCH Verlag GmbH & Co. KGaA, Weinheim

fying and general picture. Ongoing discussions incorporate various aspects, beginning with the challenge in redefining bonding and asking whether quantum mechanics or orbitals should constitute the foundation of a chemical bond.[6] The essence here is the question whether the electron density ρ is more fundamental than the wave function Ψ, which gave rise to a heated exchange of arguments.[7] However, there are several ways to describe matter at a microscopic level, and the different levels of understanding do not mutually exclude one another. Advanced models of chemical bonding should provide synergistic links between fundamentally different viewpoints; as example, Ayers and co-workers have shown how molecular-orbital theory can provide in straightforward fashion approximations to the reactivity indicators of conceptual density functional theory.[8] Other aspects that have caused disagreements relate to a different fundamental understanding of basic concepts, and the silicon–silicon triple bond has been at the center of such discussions.[9]

A refined view of chemical bonding partitions interatomic interactions into attractive orbital interaction ΔE_{oi}, Pauli repulsion ΔE_{Pauli}, and quasi-classical electrostatic interaction ΔE_{elstat}.[10] It is the interplay of these three terms that determines the bond energies and equilibrium distances of covalently bonded molecules. However, the common view of covalent bonding usually restricts the reciprocity to attractive orbital interactions between singly filled orbitals or between doubly occupied and vacant orbitals, resulting in electron-sharing bonds and donor–acceptor bonds, respectively. Further, attractive orbital interactions are often equated with the idea of orbital overlap. Repulsive interactions between electrons and in particular between electrons having the same spin are not part of the general chemistry curriculum, although the significance of repulsive forces for molecular properties such as bond strength and bond length in connection with and in relation to orbital overlap has been recognized for a long time.[11] Appreciating the importance and impact of orbital overlap for chemical bonding, Bickelhaupt and Frenking have presented a detailed analysis of chemical bonding in diatomic molecules, unifying notions derived from an analysis of orbital overlap with the concept of bond energy partitioning into ΔE_{elstat}, ΔE_{Pauli}, and ΔE_{oi}.[12] Their evaluation provides a solid basis for an assessment of the role of attractive, ΔE_{oi}, and repulsive interactions, ΔE_{Pauli}, for chemical bonding, which are both determined by the orbital overlap. Although these ideas have been perceived early on—Mulliken, for example, has pointed out that the relatively low bond energy of F_2 is due to an accumulation of non-bonded repulsion,[13] and Pitzer has stressed the importance of repulsive effects of inner shells for bonding of heavier elements[14]—they are not yet generally recognized as essentials of chemical bonding. In addition, Bickelhaupt and Frenking put special emphasis on the quasi-classical electrostatic interaction ΔE_{elstat}, an important factor that is usually not considered for covalent bonds. The authors write that "Molecules like N_2 and O_2, which are usually considered as covalently bonded, would not be bonded without the quasi-classical attraction".[12]

It appears that the epitome of chemical bonding is currently being refined and redefined. In the spirit of these ongoing developments, we set out to present a new view of an old problem, and follow a synergistic approach incorporating density descriptions and orbital approaches. At the heart of our analysis are heavy-atom analogues of acetylene, which are representatives of a class of molecules that by itself initiated a paradigm shift in main group chemistry.[2] The expansion of heavier Group 14 element chemistry not only exemplifies the synergistic cooperation between experiment and theory, but also illustrates advancement and change within basic chemical principles. Thus, we proceed with a short section in which we briefly review the development of this unusual class of compounds; the reader who is familiar with the subject or who is less interested in the historic developments might want to skip to the end of the next section and then proceed with the theoretical basis and results and discussion.

Background: The structure of tetramesityldisilene $(Ar')_2Si{=}Si(Ar')_2$, $Ar' = C_6H_2$-2,4,6-$(CH_3)_3$—the first stable compound containing a silicon–silicon double bond[15]—although a silicon analogue of ethylene, is quite different from that of typical $R_2C{=}CR_2$ molecules: Disilenes deviate from planarity, and adopt *trans*-bent geometries. Although the *trans*-bent geometries are a consequence of enhanced inter-atomic as well as intra-atomic Pauli repulsion,[16] the first-bond descriptions focused on orbital interactions only and common models of chemical bonding could not account for the unexpected geometry. Trinquier and Malrieu then derived a valence bond model for the Si=Si double bond, based on the bonding interaction of two SiH_2 fragments in their respective electronic ground states.[17] Their work may be considered as a structural extension of arguments that relate the strength of multiple bonds to the singlet–triplet separation of the interacting fragments forming the multiple bond.[18] Trinquier and Malrieu already noted that their model might also hold an explanation for the fact that some triple bonds deviate from linearity.

Whereas tetramesityldisilene relies on bulky substituents for steric protection of the reactive double-bond center, the quest for a silicon analogue of acetylene was initiated in theoretical calculations of Si_2H_2 isomers in the early 1980s,[19] shortly after the announcement of the silicon–silicon double bond. About ten years later, Colegrove and Schaefer authoritatively summarized the then current state of affairs.[20] Out of a set of eleven structures that they explored with ab initio theoretical methods, they localized four local minima on the singlet potential energy surface (PES) of Si_2H_2, depicted in Figure 1.

The *trans*-bent structure (Figure 1), which would result from a Trinquier and Malrieu analysis of Si_2H_2, represents a local minimum on the PES, but it is not the lowest energy structure. Instead, the PES analysis of Colegrove and Schaefer confirmed that the global minimum is the doubly hydrogen-bridged structure. At about the same time, experimental evidence for doubly bridged (dibridged) and singly bridged

 © 2010 Wiley-VCH Verlag GmbH & Co. KGaA, Weinheim

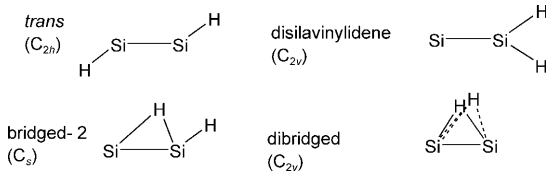

Figure 1. Local minimum valence isomers of Si_2H_2; adapted from ref. [20].

(bridged-2) structures was obtained from the submillimeter-wave rotational spectrum of disilyne.[21,22]

With the advancement of computational methodologies during the last decade of the last millennium, the heavier-atom analogues of acetylene continued to be a target for theoretical investigations. In one of the first studies that focused on more realistic model systems, Kobayashi and Nagase investigated the substituent effects on silicon–silicon triple bonds.[23] Two of the molecules considered—R-Si≡Si-R, R: Si(*t*Bu)$_3$ and Si(2,6-Et$_2$C$_6$H$_3$)$_3$—adopt a *trans*-bent geometry, and the authors followed a Trinquier and Malrieu approach in order to rationalize the deviation from linearity around the silicon–silicon triple bond.

The new millennium has witnessed the synthesis of the first stable examples of homonuclear alkyne analogues of the heavier main Group 14 elements. By now, stable heavier alkyne analogues REER have been synthesized and structurally characterized for all of the Group 14 elements, including lead (E = Pb),[24] tin (E = Sn),[25] germanium (E = Ge)[26] and silicon (E = Si).[27] We note that all of molecules display *trans*-bent structures in the solid state; dibridged molecules are not among the set of geometries that were characterized by X-ray structure analysis. A bond analysis according to Trinquier and Malrieu naturally predicts the silicon–silicon triple bond to deviate from linearity and to take on a *trans*-bent geometry.

At the same time, the experimental work continued to receive support from computational studies, and the nature of the E≡E triple bond of heavier Group 14 element alkyne analogues R-E≡E-R (R = large aryl or silyl group; E = Si–Pb) constituted a key aspect of the theoretical work undertaken. While most bond analyses are based on an orbital approach, and often used a Trinquier and Malrieu fragment analysis, Popelier and co-workers presented a study on bonding using a topological analysis of electron densities, thus complementing the Ψ approach to chemical bonding with the ρ approach.[28] The development of this intriguing field of research has been documented in various review articles,[29,30] and we refer the reader to the literature[30] for an entry into computations of R-E≡E-R molecules.

While during the recent developments in REER chemistry the unusual dibridged structure of Si_2H_2 shifted out of the focus of many research activities, the question of why the heavy-atom analogues of acetylene (E_2H_2; E = Si, Ge, Sn, Pb) exhibit unusual structures has not been forgotten. Lein, Krapp, and Frenking noticed that none of the many theoretical studies on REER systems discussed why the most stable structures of Si_2H_2, Ge_2H_2, Sn_2H_2, and Pb_2H_2 exhibit a doubly bridged geometry.[31] They then carried out density functional calculations for different E_2H_2 (E = Si–Pb) geometries and their set of isomers included a doubly bridged form **A**, a singly bridged form **B**, a vinylidene form **C**, a *trans*-bent geometry **D** as well as a linear geometry **E** (see below). The unusual structures of E_2H_2 (E = Si–Pb) were explained with the interactions between two EH moieties in their active electronic states.[31] We note that the fragment partitioning of Lein, Krapp, and Frenking resembles a Trinquier and Malrieu approach, and that their analysis bears similarities to the bonding analysis carried out for E_2H_4 molecules.[16]

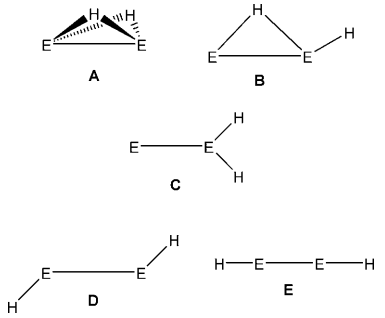

Lein, Krapp, and Frenking explain the stability ranking **A** > **B** > **D** in terms of number and type of bonding orbital contributions to the bond energy. Their investigation centers on an analysis of orbital interactions between two EH fragments and is therefore based on orbital overlap. This is one of the reasons why the vinylidene form **C** has not been considered. The atom connectivity in **C** is significantly different from that of the other isomers, thus prohibiting an analysis in terms of interacting EH fragments.

In this work, we set out to develop a unifying bond analysis approach that allows one to compare the complete set of E_2H_2 isomers on equal footing. We also address the question why dibridged structures **A**, despite the highly favorable orbital interactions, are apparently restricted to the set of E_2H_2 molecules, and are not yet observed for E_2R_2 systems. As we shall see, electrostatic interactions are essential for our argumentation.

Theoretical basis: Density functional theory constitutes the computational framework of the present work. Our calculations are based on the generalized gradient approximation (GGA), where the local density approximation, following the formulation of exchange and correlation terms according to Slater[32] and Vosko, Wilk, and Nussair,[33] respectively, is augmented by gradient corrections as prescribed by Perdew, Burke, and Ernzerhof.[34]

 © 2010 Wiley-VCH Verlag GmbH & Co. KGaA, Weinheim

Computational Methods

Computational engine: Calculations of optimized geometries and final energies were carried out with the Amsterdam Density Functional suite of programs, ADF version 2006.01.[35] Scalar relativistic effects have been incorporated according to the zero-order regular approximation (ZORA).[36] Geometries were optimized using the methodology developed by Versluis and Ziegler[37] and its relativistic extension.[38] Frequency calculations utilized an analytical implementation of perturbations due to nuclear displacements.[39] Orbitals were expanded in an uncontracted set of Slater-type orbitals, the basis sets having quadruple-ζ quality augmented by four sets of polarization functions (QZ4P).[40] Geometry optimizations made use of the frozen core approximation[41] such that each molecule was assigned a set of ten active valence electrons (QZ4Pfc). Calculations of final energies and energy partitioning analyses incorporated a full all-electron basis (QZ4Pae).

Calculations of densities used in topology analyses and calculations of systems in the presence of a background charge distribution made up of point charges have been carried out with the Gaussian03 system of programs.[42] A split-valence basis augmented by one polarization function was used for C, Si, and Ge.[43] A double-ζ basis with polarization was used for Sn.[44] Core potentials[45] were employed for Pb, using a quasi-relativistic core potential together with a corresponding double-ζ valence basis.[46] Energies of systems in the present of point charges are reported under exclusion of point charge self-energies. Topological analyses of molecular electron densities employed a modified version of the program MORPHY.[47] 3D pictures were generated using the graphical package Jmol.[48]

Bond analysis: The bond energy decomposition scheme employed in the present work,[49] widely used in the analysis of chemical bonding, is based on ideas developed by Kitaura and Morokuma[50] and by Ziegler and Rauk.[51] In order to analyze chemical bonding in a given system one separates the chemical entity into suitable fragments, which might be atomic or molecular. Then, one examines the energy of interconnection of the separated fragments associated with formation of the final molecule, which we call the instantaneous interconnection energy E_{iic}. Here, the fragments possess the local equilibrium geometry of the final molecule, and have the electronic structure that is required for bonding. E_{iic} is comprised of three major components, namely orbital interaction ΔE_{oi}, Pauli repulsion $\Delta E_{\mathrm{Pauli}}$ and quasi-classical electrostatic interaction $\Delta E_{\mathrm{elstat}}$ [Eq. (1)]:

$$E_{\mathrm{iic}} = \Delta E_{\mathrm{oi}} + \Delta E_{\mathrm{Pauli}} + \Delta E_{\mathrm{elstat}} \quad (1)$$

ΔE_{oi} contains interactions between occupied orbitals on one fragment and unoccupied orbitals on another, as well as polarization effects due to mixing of occupied and virtual orbitals on one fragment only.[52] $\Delta E_{\mathrm{Pauli}}$ refers to repulsive interactions between fragments and embodies the three- and four-electron destabilizing interactions between occupied orbitals. The energy of bonding E_{b} is obtained by adding a preparation energy term E_{prep} [Eq. (2)]:

$$E_{\mathrm{b}} = E_{\mathrm{iic}} + E_{\mathrm{prep}} \quad (2)$$

E_{prep} is the energy necessary to promote the fragments from their equilibrium geometry to the geometry in the compound, and if required, to electronically excite the fragments from their electronic ground-states to the reference states for that compound.

The different contributions to the instantaneous interconnection energy E_{iic} might be grouped together as to emphasize different aspects of chemical bonding.[53] To stress the importance of electrostatic interaction for chemical bonding, one might merge the terms for Pauli repulsion and orbital interaction into a combined orbital term ΔE^{orb}. This step can be justified keeping in mind that both terms basically stem from interactions between orbitals on different fragments; be it repulsive or attractive. The energy of bonding E_{b} then writes as follows [Eq. (3)]:

$$E_{\mathrm{b}} = \Delta E^{\mathrm{orb}} + \Delta E_{\mathrm{elstat}} + E_{\mathrm{prep}} \quad (3)$$

We refer the reader to the literature for more details on energy partitioning[10] and decomposition schemes.[54]

Density analysis: The localized-orbital locator (LOL)—introduced by Schmider and Becke[55] and referred to as ν—is based on the non-interacting kinetic-energy density τ and the charge density ρ at a given point of reference. LOL produces an intuitive measure of the relative speed of electrons in its vicinity and focuses on regions that are dominated by single localized orbitals.[56] More specific, ν is a measure of the relative value of τ in a mapping onto the finite range [0,1]. A value of $\nu = 1/2$ indicates that the kinetic energy content of the corresponding region is what would be expected from a spin-neutral electron gas of that density, and values of $\nu > 1/2$ indicate regions where electrons are localized. LOL reflects common chemical concepts such as atomic shells, molecular bonds, and lone-pair regions in a clear and intuitive manner.[55] We also note that the kinetic energy density τ contains pertinent information in the description of Pauli repulsion.[57]

Ideas borrowed from the topological analysis of electron charge density[58] allow one to locate critical points and in particular (3,−3) attractors Γ in the gradient vector field of LOL.[59] The Γ topology of LOL and its associated ν_Γ values contain valuable information of bond covalency,[60] but here we focus on the fact that the Γ topology also recovers localization patterns of core electrons.

Results and Discussion

What C_2H_2 and all E_2H_2 (E = Si–Pb) molecules have in common is an interconnected C–C or E–E core unit and a set of ten valence electrons. Different spatial arrangements of the two hydrogen atoms then result in various isomeric structures, such as dibridged **A**, bridged **B**, vinylidene **C**, *trans*-bent **D**,, and linear **E**. Thus, we optimized geometries of C_2^{2-} **1**, Si_2^{2-} **2**, Ge_2^{2-} **3**, Sn_2^{2-} **4**, and Pb_2^{2-} **5**, as well as geometries for isomers **A**–**E** of C_2H_2 **1a**, Si_2H_2 **2a**, Ge_2H_2 **3a**, Sn_2H_2 **4a**, and Pb_2H_2 **5a**.

The stability ranking of isomers **A**–**E** for C_2H_2 and E_2H_2 (E = Si–Pb) is one the central themes of the present work; in Table 1 we report total energies for all structures considered. Since the unusual dibridged isomer **A** plays a particular and special role, the energies in Table 1 are presented as relative total bond energies ΔE_{b} with respect to structure **A**. Lein, Krapp, and Frenking have performed a similar comparative energy assessment,[31] and for the sake of comparison, their energy data are also included in Table 1.

Our results are in full qualitative accordance and in good quantitative agreement with the results of Lein, Krapp, and Frenking. Minor differences in ΔE_{b} are most likely due to the fact that the two studies utilize different pure density functionals (BP86 vs. PBE). They discuss in much detail the energy ranking and the geometries of the full set of E_2H_2 molecules (E = Si–Pb), and they put their theoretical values at BP86/QZ4P in context and comparison to other experimental and high-level computational work.[31] Thus, we restrict ourselves to essential aspects that will be of importance for our further discussion.

What differentiates C_2H_2 and E_2H_2 (E = Si–Pb) is a reversal in stability ranking of isomers **A**–**E**. It comes as no surprise that the most stable isomer for C_2H_2 is acetylene **1a** **E**,

 © 2010 Wiley-VCH Verlag GmbH & Co. KGaA, Weinheim

Table 1. Relative total bond energies ΔE_b (in kJ mol^{-1}) of isomers **A–E** for molecules **1a–5a**.

	BP86/QZ4P[a]	PBE/QZ4Pae//PBE/QZ4Pfc[b]	#IF[c]
1aA	–[d]	0	1
1aB	–[d]	−133	0
1aC	–[d]	−130	0
1aD	–[d]	−296	0
1aE	–[d]	−320	0
2aA	0	0	0
2aB	41	42	0
2aC	64	69	0
2aD	83	87	0
2aE	174	174	2
3aA	0	0	0
3aB	46	45	0
3aC	69	68	0
3aD	93	91	0
3aE	233	227	2
4aA	0	0	0
4aB	57	57	0
4aC	81	81	0
4aD	106	107	0
4aE	270	268	2
5aA	0	0	0
5aB	71	71	0
5aC	113	114	0
5aD	130	130	0
5aE	387	389	2

[a] Ref. [31]. [b] This work. [c] Number of imaginary frequencies. [d] Not reported.

and the five C_2H_2 isomers considered in this work rank in terms of stability as **E** > **D** > **C** > **B** > **A**. For E_2H_2 (E = Si–Pb), our calculations confirm the by now well-known fact that the dibridged isomers are most stable, and the stability ranking of the five E_2H_2 isomers is inverted, **A** > **B** > **C** > **D** > **E**. Also reported in Table 1 is the number of imaginary frequencies for each isomer of each molecule. All but the least stable isomers constitute local minima on their respective PES. For C_2H_2, isomer **A** describes a transition state for interconversion of two isostructural vinylidene forms **C**, whereas for E_2H_2 molecules, isomers **E** having two degenerate negative frequencies describe transition states for interconversion of isostructural *trans*-bent geometries **D**. Interconversion pathways and molecular displacements at the transition state are illustrated in Scheme 1.

The data of Table 1 clearly indicate that there seems to be an essential qualitative difference in bonding of C_2H_2 and E_2H_2 (E = Si–Pb). The most stable C_2H_2 isomer **E** represents a transition state on the PES of E_2H_2 systems, and the most stable E_2H_2 isomer **A** represents a transition state on the PES of C_2H_2.

The cardinal change in structure and reactivity when going from the first long row to higher rows has long been recognized as one of the indispensable conceptions underlying the periodic table. In his treatise on chemical bonding in higher main group elements, Kutzelnigg puts special emphasis on the essential difference between the atoms of the first long row and those of higher rows.[61] The fact that the cores of the former contain only s orbitals, whereas the cores of the latter include at least s and p orbitals is responsible for deviations in structure and reactivity of elements of the first long row from those of higher row elements. We will comment on the influence of extended electronic cores in more detail in our next section.

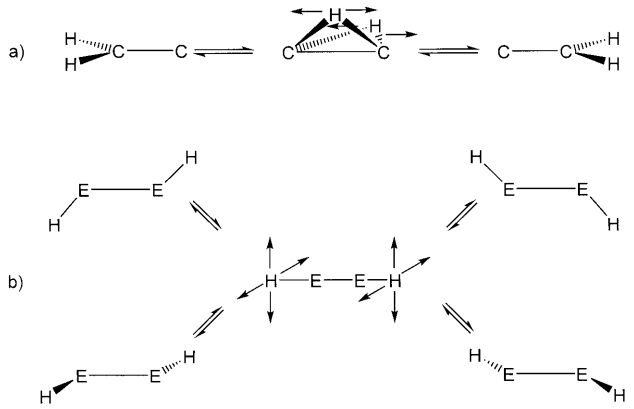

Scheme 1. Molecular displacements at the transition state for a) C-A$^+$-C interconversion in C_2H_2, and for b) D-E$^+$-D interconversion in E_2H_2 (E = Si–Pb).

Core electrons and electrostatic interactions: Since the localized orbital locator is indicative of details of not only molecular, but also atomic electronic structure,[55] an analysis of the LOL topology should reveal the essential differences between carbon and its heavier homologues, namely electronic cores without and with p orbitals. As an exemplarily analysis, we present a qualitative assessment of LOL profiles of **1**, **1aA**, **2**, AND **2aA**. The location and orientation of (3,−3) attractors Γ and associated ν_Γ values are depicted in Figure 2.

Molecules **1** and **2** contain the essential features of C_2H_2 and Si_2H_2 isomers: an interconnected C–C or Si–Si unit and

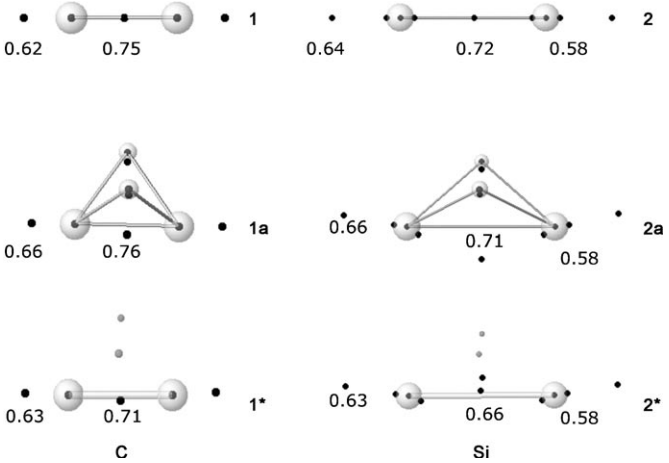

Figure 2. (3,−3) Attractors Γ (black circles) and associated ν_Γ values for **1** and **2**, and for **A** isomers of **1a**, **1***, **2a**, and **2***. Bond lines between atoms are derived from standard geometric connectivity arguments; atoms are displayed as translucent spheres with a 10% van der Waals radius. Point charges in **1*** and **2*** are indicated as gray circles.

 © 2010 Wiley-VCH Verlag GmbH & Co. KGaA, Weinheim

a set of ten valence electrons. Each nucleus position is associated with one attractor Γ due to the 1s electronic core, but LOL also features attractors between bonded C–C and Si–Si atoms with ν_Γ values of 0.75 and 0.72, respectively. Molecular regions associated with lone pairs are characterized by an attractor Γ with a ν_Γ value around 0.63. What significantly differentiates the LOL profile of **2** from that of **1** is the presence of additional core attractors due to the extended electronic core comprising additional 2s and 2p orbitals. The presence of p orbitals allows for a polarization of the second shell of core electrons; for **2**, two additional Γ attractors with $\nu_\Gamma = 0.58$ are found close to each nucleus, located along the line connecting the two lone pair attractors.

The LOL profiles around the H atoms in **1aA** and **2aA** carry characteristics of a 3c–2e bond,[62] but it is the displacement of the lone pair and second core shell attractors that differentiates the electronic structure around the C–C unit in **1a A** from that of the Si–Si unit in **2aA**. The core and lone pair polarization is more pronounced in **2aA** than it is in **1aA**, and the presence of a p orbital core is responsible for this effect.

The lone pair and second core shell polarization is caused by electrostatic interactions between the extended electronic core and the additional H nuclei; the expansion of the valence space has only a minor influence. To illustrate this point, we have calculated LOL profiles for **1*** and **2***: C_2^{2-} and Si_2^{2-} molecules that possess the C–C and Si–Si core of **1aA** and **2aA** where the electron density is polarized due to the presence of a background charge distribution that is made up of two protonic point charges placed at the position of the H atoms in **1aA** and **2aA**. The location and orientation of (3,−3) attractors Γ and associated ν_Γ values for **1*** and **2*** are also depicted in Figure 2, and an inspection of Figure 2 shows that the LOL profile of the core and lone pair regions of the kinetic energy density is qualitatively identical for **1a A** and **1*** as well as for **2aA** and **2***. Thus, the lone pair and second core shell polarization is indeed due to the presence of electrostatic interaction. Electrostatic interactions also influence the valence electron density; the Γ attractor in **2a A** with $\nu_\Gamma = 0.71$ is split into two Γ attractors in **2*** which are substantially displaced toward the position of the point charges. We will develop a more extended and detailed bond analysis in the next section of our discussion, but our qualitative LOL analysis illustrates the role of electrostatic interactions, and traces the difference between C_2H_2 and E_2H_2 systems to the essential difference of an extended electronic core that besides s orbitals comprises at least one set of p orbitals.

To obtain a more quantitative assessment of the influence of electrostatic interactions on the valence and core densities of C_2H_2 and E_2H_2 (E = Si–Pb) systems, we analyzed the total energies of isomers **A**–**E** for systems ***n****, ***n*** = 1–5. Here, a system ***n**** contains the Group 14 atom arrangement and the same number of electrons as the related **na** molecule, and a background charge density of two protonic charges has been included, the point charges placed at the H-atom positions of the corresponding **na** molecules. Since the emphasis is on the electronic structure of **na** systems, the point charge self energy has been excluded from the total energies of **n*** systems. Since the dibridged isomer **A** occupies a special role in our discussion, total energies are given as relative total energies ΔE_{tot} with respect to structure **A**. The results of our analysis are presented in Figure 3.

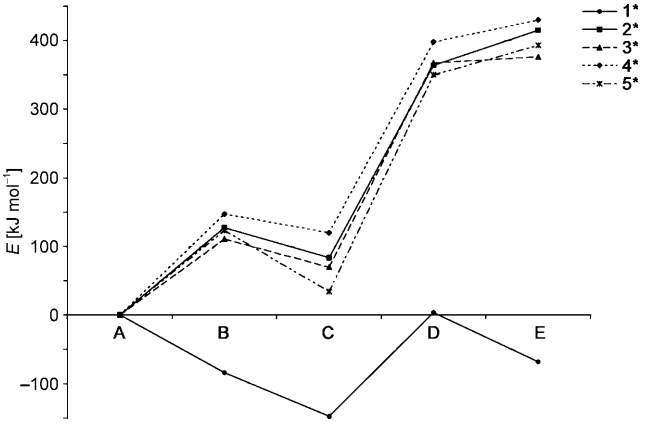

Figure 3. Relative total energies of **1***–**5*** for isomers **A**–**E** with respect to structure **A**.

The influence of the positive background charge generally lowers the total energy of X_2^{2-} (X = C–Pb) systems, but for E_2H_2 (E = Si–Pb) molecules, we note that this charge stabilization is most efficient for structure **A**. On the contrary, for C_2H_2 the charge stabilization is least efficacious for isomer **A**. Following our LOL analysis, we explain this by a polarization of the extended electronic core that leads to an enhancement in electrostatic interaction for the heavier elements Si, Ge, Sn, and Pb. For these atoms, the general stability trend already observed by Lein, Krapp, and Frenking—**A** > **B** > **D**—is reflected in the energy ranking of isomers **A**, **B**, **D** for molecules **2***–**5***. This is an indication of the importance of electrostatic interaction particularly for the heavier Group 14 atoms. The relative energies of the vinylidene structure **C** of **2***–**5***, however, do not line up with the energy ranking found for molecules **2a**–**5a**. Clearly, the skeletal arrangement in which two H atoms are only connected to the same E atom leads to a different bonding situation that we will analyze in more detail in the next section. However, for the two pairs of related isomers—**A**, **B** and **D**, **E**—the relative stabilities calculated for E_2H_2 (E = Si–Pb) molecules—**A** > **B** and **D** > **E**—are reproduced, and isomers **E** of **2***–**5*** are at highest energies.

The fact that vinylidene structure **C** seems to fall out of previously established energy rankings, and to be particularly favored for **1* C**, which is derived from $C{=}CH_2$, implies that the interaction between the valence density and the positive background charge also induces a stabilizing effect. We further note that isomer **C** is indeed different from isomer pairs **A** and **B** as well as **D** and **E**, and this observation holds true for both C_2H_2 as well as E_2H_2 systems. While the influence of electrostatic interactions on core orbitals

 © 2010 Wiley-VCH Verlag GmbH & Co. KGaA, Weinheim

provides a first valuable assessment of relative energies, the bonding character of X_2H_2 (X = C–Pb) molecules cannot easily be reduced to one bonding aspect only, and a more detailed bond analysis of X_2H_2 systems will provide a clearer explanation and a more comprehensive picture.

Bond analysis: In order to evaluate the bonding situation in different isomers of X_2H_2 (X = C–Pb), we have used a fragment based energy decomposition scheme as outlined in the context of our theoretical basis. Our fragment analysis differs from the one employed by Lein, Krapp, and Frenking in that we do not reduce bonding in E_2H_2 molecules to proper coupling of two EH fragments. Instead, we base our analysis on the similarities—an interconnected X–X core and a set of ten valence electrons—as well as the differences—distinctive spatial arrangement of H atoms—of various isomers of X_2H_2 (X = C–Pb) molecules. Whereas their analysis excluded the vinylidene isomers **C** because the connectivity $E–EH_2$ prohibits a breakdown into two EH fragments,[31] our analysis represents a unified approach that allows for a comparison of isomers **A**–**E** including **C** on an equal footing. We partition the various isomers **A**–**E** of X_2H_2 (X = C–Pb) molecules in one X_2^{2-} fragment and one $(H\cdots H)^{2+}$ fragment as outlined in Equation (4).

$$X_2^{2-} + (H\cdots H)^{2+} \rightarrow X_2H_2 \quad E_b \tag{4}$$

This analysis might not give direct answers to questions as to the bond character of the X–X multiple bond, it is, however, expected that the analysis will provide answers to the cardinal question why heavy-atom analogues of acetylene (E_2H_2; E = Si–Pb) exhibit unusual structures. For this reason, we present relative energies ΔE_b and a relative energy partitioning, $\Delta\Delta E_{elstat}$ and $\Delta\Delta E_{oi}$, with respect to isomers **A** of molecules **1a**–**5a**. Since hydrogen does not possess any electronic core, the fragment analysis as outlined in Equation (4) does not contain any contributions due to Pauli repulsion, and for molecules **1a**–**5a**, the bond analysis yields identical contributions to $\Delta\Delta E_{oi}$ and $\Delta\Delta E^{orb}$. Results of our bond analysis are collected in Table 2.

A first brief inspection of the data presented in Table 2 leads to the following three key observations: 1) For each of the molecules **1a**–**5a**, the most stable isomer possesses the strongest electrostatic interaction. 2) Differences in the preparation energy ΔE_{prep} for isomers **A**–**E** for a given molecule amount to a sizeable portion of the relative energies of bonding ΔE_b, but for any given isomer, the differences in preparation energy ΔE_{prep} are similar for molecules **1a**–**5a**. 3) For all molecules, isomers **C** are least favored in terms of ΔE_{elstat}, but are most favored in terms of ΔE_{oi} or ΔE^{orb}.

In the following, we present qualitative arguments that serve as basis to rationalize these trends. Since bond lengths d_{X-H} and substituent separations d_{H-H} are main components of our syllogism, relevant geometric parameters are collected in Table 3.

Table 2. Contributions to the relative instantaneous interconnection energy ΔE_{iic} of $X_2^{2-}$and $(H\cdots H)^{2+}$ fragments, preparation energies, and total bond energies (in kJ mol^{-1}) for the formation of isomers **A**–**E** of molecules **1a**–**5a** with reference to structure **A**.

	$\Delta\Delta E_{elstat}$	$\Delta\Delta E_{oi}$; $\Delta\Delta E^{or}$[b]	ΔE_{prep}	ΔE_b[a]
1aA	0	0	0	0
1aB	−26	25	−131	−133
1aC	169	−213	−85	−130
1aD	−46	157	−407	−296
1aE	−95	163	−387	−320
2aA	0	0	0	0
2aB	47	152	−156	42
2aC	244	−27	−149	69
2aD	206	278	−397	87
2aE	68	490	−383	174
3aA	0	0	0	0
3aB	80	110	−145	45
3aC	257	−74	−115	68
3aD	228	243	−379	91
3aE	136	454	−362	227
4aA	0	0	0	0
4aB	68	128	−139	57
4aC	232	−42	−109	81
4aD	205	251	−349	106
4aE	89	493	−314	268
5aA	0	0	0	0
5aB	81	116	−130	67
5aC	216	−21	−86	109
5aD	200	261	−335	126
5aE	71	567	−252	386

[a] Obtained as $\Delta\Delta E_{elstat}+\Delta\Delta E_{oi}+\Delta E_{prep}$.

In a first approximation, the strength of the electrostatic interaction can be estimated by evaluating the distance d_{X-H} between the protonic charges and the X atoms (X = C–Pb) as central points of the valence electron density. Of further importance is the fact whether both X centers or only one X atom is positioned in close vicinity to a positive charge center, or—in other words—whether one X atom or both X centers are bonded to H. Comparing corresponding data presented in Tables 2 and 3, we find that for the **A**, **B**, **D**, and **E** isomers of **1a** ΔE_{elstat} correlates well with d_{C-H}: acetylene possesses the shortest C–H—calculated as 107 pm—and exhibits the strongest electrostatic interaction, whereas the dibridged isomer **A** displays the longest C–H bonds of 129 pm, and represents the isomer with the smallest electrostatic interaction. The fundamentally different bonding pattern in isomer **C** is reflected in its especially small ΔE_{elstat}

Table 3. X–H distances d_{X-H} (in pm) and changes in H–H separations Δd_{H-H} with respect to isomer **A** (in pm) for isomers **A**–**E** of molecules **1a**–**5a** (X = C, Si, Ge, Sn, Pb).

	d_{X-H}					Δd_{H-H}				
	A	**B**	**C**	**D**	**E**	**A**	**B**	**C**	**D**	**E**
1a	129	134–122, 108	110	109	107	0	32	19	168	166
2a	169	172–166, 151	150	151	147	0	57	52	259	295
3a	184	188–178, 159	157	159	151	0	52	39	267	297
4a	202	204–200, 177	176	178	169	0	66	48	315	344
5a	214	215–210, 187	186	189	174	0	66	38	339	344

© 2010 Wiley-VCH Verlag GmbH & Co. KGaA, Weinheim

contribution. The positive charges of the $(H\cdots H)^{2+}$ ligand are in close vicinity to electrons centered around only one of the two carbon atoms, and the electrostatic charge attraction is therefore least for isomer **C**.

Similar qualitative arguments apply to the isomers of **2a–5a**, with the notable exception of isomers **A**. Despite the fact that isomers **A** display the largest X–H separations, we observe for Group 14 elements beyond the first long row the largest ΔE_{elstat} contribution. We have to keep in mind that ΔE_{elstat} represents a quasi-classical attraction, and the LOL analysis reveals how polarization of the extended electronic core might lead to an enhancement of electrostatic interaction of the core electron density within a positive electric field. Part of the answer to the question as to why do the heavy-atom analogues of acetylene (E_2H_2; E = Si–Pb) exhibit unusual structures is certainly the extended electronic core that besides s orbitals comprises at least one set of p orbitals. In the next section, we will see that this argument is supplemented by special characteristics of the H substituent. The reversal of the stability ranking of isomers **A–E** when proceeding from C_2H_2 isomers to E_2H_2 (E = Si–Pb) isomers is due to an extended electronic core of the E elements, but we will see that the fact that dibridged structures so far have been characterized for hydrogen systems only is related to properties of the H substituents and does not depend on the nature of the 14 element.

Within our fragment partitioning, the major contribution to the preparation energy ΔE_{prep} is due to electrostatic repulsion between two protons which are brought from infinite separation to a close positioning that resembles the geometric arrangement of H atoms in the final molecule. Thus, the preparation energy too is dominated by electrostatic interactions. Minor contributions to ΔE_{prep} arise from changes in X–X bond length, going from the free X_2^{2-} unit to the (X)(X) arrangement in the final molecule. Since relative changes in H–H separation between isomers **A–E** of molecules **1a–5a** are similar (compare Table 3), the differences in preparation energy ΔE_{prep} are analogous for molecules **1a–5a** (compare Table 2).

In order to elucidate the special role of isomer **C**, we investigate the change in orbital interaction for isomers **A–E** of molecules **1a–5a** (see Table 2). We find that isomer **C** is generally favored in terms of ΔE_{oi}, and that this preference is most dominant for C_2H_2 **1a**. Within our fragment partitioning, ΔE_{oi} relates to an expansion of the variational space occupied by the valence electron density, and for all X_2H_2 molecules (X = C–Pb), this stabilizing orbital interaction is largest for isomer **C**. The following simple Lewis-structure argument, constructed in Scheme 2, provides an innate explanation.

The valence space of X_2^{2-} that comprises three electron groups (one X–X multiple bond and two lone pairs) is expanded to four electron groups (one X–X multiple bond, two X–H bonds and one lone pair) when the X_2^{2-} core unit combines with the $(H\cdots H)^{2+}$ ligand to form the vinylidene-like isomer **C**. On the other hand, formation of acetylene-like isomers **E** or **D** does not lead to an increase in the number of electron groups. Similar arguments hold for the bridged isomers **B** and **A**, which possess one or two 3c–2e XHX bonds that each constitutes one electron group.

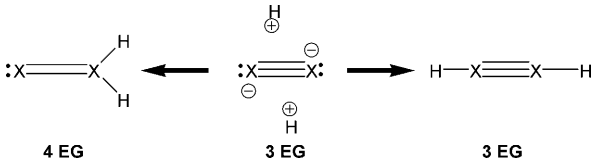

Scheme 2. Lewis structures revealing the presence of three electron groups (3 EG) in X_2^{2-} and in acetylene-like structures, and four electron groups (4 EG) in vinylidene-like structures.

So far, we have seen that part of the answer to the question posed by Lein, Krapp, and Frenking can be found within the extended electronic core of the heavier Group 14 elements Si–Pb. But the special nature of the hydrogen substituent plays an equally important role in formulating a well-founded answer. The H substituent does not possess an electronic core, and our fragment partitioning does not have contributions due to Pauli repulsion. This situation will change when we move on to other substituents that have an electronic core and bonding-inactive electrons. In this context, the first evidence for a species containing a genuine Si–Si triple bond was presented in 1986 by West and co-workers,[63] who described a thermolysis reaction providing the synthetic equivalent of dimethyldisilyne MeSi≡SiMe. The first ab initio calculations on Si_2Me_2 carried out by Schaefer and co-workers revealed that this molecule is very different not only from its carbon analogue C_2Me_2, but also from its parent compound Si_2H_2.[64] The silylidene structure $Si{=}SiMe_2$ was found to constitute the isomer at lowest energies. The low-lying isomer **A** for Si_2H_2 converted into a high-lying isomer for Si_2Me_2, partially due to steric interference of the bridging methyl groups. The authors concluded that the behavior of Si_2Me_2 cannot be simply predicted from that of Si_2H_2.[64] Although the silylidene isomer of Si_2Me_2 does not contain a Si–Si triple bond, extended calculations by Colegrove and Schaefer identified *trans*-dimethyldisilyne MeSi≡SiMe as an achievable synthetic target.[65] We will conclude our work with a brief analysis of extended Si_2R_2 systems that eventually furnished the first stable compound containing a silicon-silicon triple bond.[27]

Extended Si_2R_2 systems: We have explored the potential energy surface of Si_2Me_2 **2b** guided by the isomer manifold **A–E** depicted above. As it was the case for Si_2H_2 **2a**, isomer **E** has two degenerate negative frequencies and describes the transition state for interconversion of isostructural *trans*-bent geometries **D**. Our efforts to localize a singly-bridged isomer **B** were not successful and converged to the silylidene isomer **C** in facile fashion. Attempts to localize a dibridged isomer **A** resulted in new a structure that so far has not been considered, namely a twisted isomer **F** that exhibits C_2 symmetry. Isomer **F** resembles features of the twist conformer (Figure 4, top)) of Si_2H_2 discussed by Colegrove and

 © 2010 Wiley-VCH Verlag GmbH & Co. KGaA, Weinheim

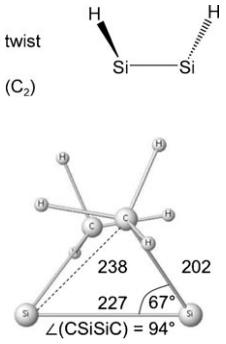

Figure 4. Twist conformer of Si_2H_2 (top: adapted from ref. [20]) and the twisted isomer **F** of Si_2Me_2 (bottom: optimized PBE/QZ4Pfc geometry; bond lengths in pm).

Schaefer,[20] and these two structures are displayed in Figure 4.

The existence of a local minimum with twist geometry on the potential energy surface of Si_2H_2 was subject of some discussion, but Colegrove and Schaefer established that the twist conformer (see Figure 4, top) collapses smoothly and without barrier to the dibridged minimum (compare Figure 1).[20] On the other hand, when comparing Si_2H_2 and Si_2Me_2, it was mentioned early on that the most noticeable change is the destabilization of the dibridged isomer,[64] presumably due to steric interaction or Pauli repulsion caused by the two methyl groups. We further point out that isomer **F** bears resemblance to the global minimum structure reported for Pb_2Ph_2.[66]

Of the three local minimum structures **C**, **D**, and **F**, dimethyldisilavinylidene $Si{=}Si(Me)_2$ represents the global minimum geometry, followed by *trans*-dimethyldisilyne MeSi≡SiMe being 15 kJ mol^{-1} higher in energy. The twist isomer **F** is positioned 22 kJ mol^{-1} above isomer **C** on the potential energy surface. We also have used a bond analysis to reveal essential differences between the bonding of isomers **C**, **D**, and **F** of Si_2Me_2 **2b**, and we partitioned the three isomers **C**, **D**, and **F** in one Si_2^{2-} fragment and one $(H_3C{\cdots}CH_3)^{2+}$ fragment as outlined in Equation (5).

$$Si_2^{2-} + (H_3C \cdots CH_3)^{2+} \rightarrow Si_2(CH_3)_2 \; E_b \qquad (5)$$

Thus, we followed essentially the same protocol as described above for Si_2H_2 isomers. The results of our bond analysis of various Si_2Me_2 isomers are collected in Table 4.

Table 4. Contributions to the relative instantaneous interconnection energy ΔE_{iic} of $Si_2^{2-}$and $(CH_3{\cdots}CH_3)^{2+}$ fragments, preparation energies, and total bond energies (in kJ mol^{-1}) for the formation of isomers **C**, **D**, **F** of molecule **2b** with reference to structure **C**.

	$\Delta\Delta E_{Pauli}$	$\Delta\Delta E_{oi}$	$\Delta\Delta E^{orb}$	$\Delta\Delta E_{elstat}$	ΔE_{prep}	ΔE_b[a]
C	0	0	0	0	0	0
D	−103	317	214	−26	−173	15
F	428	−145	283	−336	75	22

[a] Obtained as $\Delta\Delta E^{orb}+\Delta\Delta E_{elstat}+\Delta E_{prep}$.

What differentiates the bonding analysis for Si_2Me_2 from that of Si_2H_2 is the presence of contributions due to Pauli repulsion. The $(CH_3{\cdots}CH_3)^{2+}$ fragment possesses Si–CH_3 bonding-inactive electrons—the electronic core of the carbon atoms as well as electrons within the C–H bonds—, which give rise to Pauli repulsion between the two bond forming fragments, commonly referred to as a steric effect. We further note that contributions due to intra-fragmental Pauli repulsion between the two methyl groups constitute a major part of the preparation energy E_{prep}.

Like the dibridged **A** isomers of E_2H_2 (E = Si–Pb), the twist isomer **F** of Si_2Me_2 is highly favored in terms of quasi-classical electrostatic interaction ΔE_{elstat}, and it is the balance between stabilizing electrostatic interaction and destabilizing Pauli repulsion that establishes the overall stability ranking of a twist isomer **F**. We have seen before that polarization of the extended electronic core leads to an enhancement in electrostatic interaction for the heavier Group 14 elements. Thus, one might hypothesize that for the heaviest E_2R_2 systems having the largest electronic core, the bonding electrostatic forces might outweigh the antibonding Pauli repulsion and convert the twist isomer **F** into the global minimum structure—a hypothesis that is in accord with the results of calculations of Pb_2Ph_2.[66]

Of special interest is a comparison between the silylidene isomer **C** and the *trans*-bent geometry **D**. The silylidene structure is highly favored in terms of orbital interactions ΔE_{oi}, whereas the *trans*-bent geometry **D**, due to a larger separation of the two methyl substituents, is highly favored in terms of ΔE_{Pauli} and ΔE_b. It is most important to realize that $\Delta\Delta E_{oi}$ and $\Delta\Delta E_{elstat}$ for the transition **C** → **D** are similar for Si_2H_2 **1a**—305 and −38 kJ mol^{-1}—and Si_2Me_2—317 and −26 kJ mol^{-1}, respectively. With expansion of the steric demand of substituents R in Si_2R_2, we would expect that the differences in ΔE_{oi} and ΔE_{elstat} between isomers **C** and **D** remain similar, whereas isomer **D** becomes increasingly favored in terms of ΔE_{Pauli}. Eventually, the increase in Pauli repulsion will render the *trans*-bent isomer **D** the global minimum structure at lowest energy. These considerations reflect the essence of the theoretical work carried out by Nagase and co-workers: "stable silicon–silicon triply bonded compounds are synthetically accessible when they are properly substituted".[67] Nagase refers to the transformation that converts disilynes RSi≡SiR into disilavinylidenes Si=SiR_2 as 1,2-R shift, and it is important to prevent the 1,2-R shift in RSi≡SiR to maintain a disilyne structure.[68]

Reaction energies for the 1,2-R shift of various Si_2R_2 molecules are collected in Table 5; negative values indicate a preference for the disilavinylidene isomer, whereas positive values reveal that the disilyne constitutes the more stable

Table 5. Reaction energies for the 1,2-R shift RSi≡SiR → Si=SiR_2 (in kJ mol^{-1}).

R	B3LYP/3-21G*[a]	PBE/QZ4Pae//PBE/QZ4Pfc[b]
H	−33	−18
Me	−29	−15
SiH_3	−23	–
$SiMe_3$	−15	–
Si*t*Bu$_3$	41	–
SiDep$_3$[c]	50	–

[a] Ref. [23]. [b] This work. [c] Dep = 2,6-$Et_2C_6H_3$.

© 2010 Wiley-VCH Verlag GmbH & Co. KGaA, Weinheim

isomer. We present results from the work of Nagase,[23] as well as results obtained in the present work.

For small substituents, R = H or Me, the calculations indicate that the disilavinylidene constitutes the more stable isomer. The numeric discrepancy between data presented by Nagase and data of the present work is most likely due to differences in the basis sets employed, but the general trend of the B3LYP/3-21G* calculations—the preference for the disilavinylidene decreases by about 3-4 kJ mol^{-1} when H is substituted by Me—is well reproduced by the PBE/QZ4Pae//PBE/QZ4Pfc calculations. As we have deduced from our bond analysis, the difference in Pauli repulsion governs the preference for a disilyne over a disilavinylidene structure, and an expansion of the steric bulk of the R substituent should render the disilyne geometry the global minimum structure. This is in accord with the calculations of Nagase (compare Table 5); compounds with large, sterically demanding substituents such as tBu$_3$Si-Si≡Si-SitBu$_3$ and Dep$_3$Si-Si≡Si-SiDep$_3$ (Dep = 2,6-Et$_2$C$_6$H$_3$) were predicted to adapt a disilyne ground state geometry. In a later study, Nagase elaborated on this idea and came to the conclusion that it can be "expected that disilynes will be soon synthesized and isolated as stable triply bonded compounds".[68] Three years later, this theoretical prediction became reality with the synthesis and characterization of 1,1,4,4-tetrakis-[bis(trimethylsilyl)methyl]-1,4-diisopropyl-2-tetrasilyne, the first stable compound with a silicon-silicon triple bond.[27]

Conclusion

The results obtained in this work allow us to formulate an answer to the question why the energetically lowest lying structures of the heavier homologues of acetylene exhibit the unusual hydrogen-bridged geometries. Electrostatic interactions are essential in our argumentation. We looked at the bonding in X_2R_2 molecules (X = C–Pb) in terms of interaction of two fragments, the core fragment X_2^{2-} of two Group 14 elements and the substituent fragment $(R\cdots R)^{2+}$. If the Group 14 element possesses an extended electronic core that comprises at least one set of p orbitals, then the electrostatic interaction ΔE_{elstat} between the X_2^{2-} core fragment and the positively charged substituent fragment is strongest in case of the dibridged structure **A**, which also effects the relative strength of the instantaneous interconnection energy ΔE_{iic}. Therefore, heavier homologues of acetylene but not acetylene itself might display a preference for the dibridged structure **A**.

A propensity in the instantaneous interconnection energy E_{iic} turns into a preference in bond energy E_b only if E_{iic} can favorably compensate for the preparation energy E_{prep} of the fragments $(R\cdots R)^{2+}$, which is governed by repulsive interactions of the two positively charged R^+ substituents. Despite the fact that the R^+ substituents come closest within the dibridged isomer **A**, the fragmental preparation energy in E_2H_2 (E = Si–Pb) can be overcome by E_{iic}, since H^+ does not possess an electronic core nor any bonding-inactive electrons. As a consequence, E_{prep} does not contain any contributions due to Pauli repulsion ΔE_{Pauli}, but is dominated by intra-fragmental electrostatic repulsion. The situation changes for substituents R that have an electronic core and bonding-inactive electrons, such as a methyl substituent CH_3. For Si_2Me_2, not only does the dibridged structure **A** no longer constitute the global minimum geometry, the dibridged arrangement distorts into the twist geometry **F**.

Our answer to the question posed above contains two equally important parts. The heavier homologues of acetylene E_2H_2 (E = Si–Pb) exhibit hydrogen-bridged geometries **A** because the extended electronic core with at least one set of p orbitals of the Group 14 elements beyond the first long period is responsible for favorable electrostatic E–H interactions, being the strongest for **A** when compared to the other isomers, and because the H substituent does not posses an electronic core nor any bonding-inactive electrons which would give rise to a significant amount of Pauli repulsion. When one of two criteria is not met—the carbon atoms in C_2H_2 do not possess an extended electronic core; the methyl substituents in Si_2Me_2 do posses an electronic core and bonding-inactive electrons—the unusual dibridged structure no longer constitutes the energetically preferred geometry. Not only can the behavior of Si_2H_2 not be anticipated from that of C_2H_2, the behavior of Si_2Me_2 too cannot be simply predicted from that of Si_2H_2. Our argumentation is not based on orbital arguments that most often provide the basis for explanations of phenomena of chemical bonding, but is based on electrostatic interactions and Pauli repulsion, two interactions that gain increasing importance in refined views of chemical bonding.[12] E_2H_2 molecules would not adapt a dibridged structure without the quasi-classical electrostatic attraction due to an extended electronic core of the E atoms. Further, E_2H_2 molecules would not adapt a dibridged structure without the absence of an electronic core of the H atoms.

The very problem has been addressed before by Lein, Krapp, and Frenking, who based their answer on the bond-formation process of two EH (E = Si, Ge, Sn, Pb) fragments in their electronic ground state and in their first excited state.[31] They noticed that it is only the combination of two EH fragments in the first excited state that leads to the standard Lewis-type structure with a linear arrangement HE≡EH, and that the interaction between EH fragments in the ground state explains the preference for the hydrogen-bridged geometries. They concluded that acetylene differs from its heavier homologues, because it takes much less energy to excite CH from the ground state to the excited state than for the heavier species, and that only in the carbon compound does the stronger bonding in the linear form HC≡CH compensate for the excitation energy of the fragments EH.[31] While our investigation focuses on electrostatic interactions and Pauli repulsion, the Lein, Krapp, and Frenking analysis puts an emphasis on orbital interactions. While our evaluation is based on stabilization of a given valence space density, their analysis is based on the creation of a valence space orbital manifold. In a way, their analysis designates

 © 2010 Wiley-VCH Verlag GmbH & Co. KGaA, Weinheim

the wave function as the foundation of chemical bonding, whereas our exploration realizes the importance of electron densities. Both approaches are valid in their own right, but a few aspects that are only implicitly considered in their analysis are explicitly expressed in the present work. The fact that the excitation energy of EH (E = Si–Pb) is significantly higher than for CH is a consequence of intra-atomic Pauli repulsion,[16] and thus directly related to the extended electronic core of Si, Ge, Sn, and Pb. The analysis presented by Lein, Krapp, and Frenking for E_2H_2 molecules intuitively leads to the assumption that the bonding patterns might be extended to E_2R_2 systems. Whether ER fragments such as $SiCH_3$ are or are not, due to an expected high geometric preparation energy, suitable fragments for a bond analysis, it is a fair assumption that they would display high excitation energies like SiH and possess the requirements to form dibridged structures. Only a detailed analysis of the results obtained from an EH fragment partitioning will reveal the relative importance of $\Delta E_{\mathrm{Pauli}}$.

Our bond analysis is guided by results of an examination of the kinetic energy density τ by means of the localized orbital locator LOL. The investigation of patterns in kinetic energy of a system in turn delivers valuable insight into bond covalency,[59,60] a concept being central to what is commonly understood as the chemical bond. Therefore, the bond analysis presented in this work unifies wave function concepts and ideas derived from electron densities into an extended description of the chemical bond.

Questions that are not directly addressed in the present work relate to the E–E bond multiplicity in REER systems, which have caused controversial discussion in the literature. Intuitively, one could describe the bonding in all REER isomers investigated in this work as variation of the triple bond theme in the sense of a Lewis structure description. However, not all triple bonds are alike in character, and one of the concepts that is often more or less successfully applied in characterizing chemical bonds is the bond order. For systems such as the ones discussed here, Landis and Weinhold have recently employed natural bond orbital-based analyses to quantify molecular bond orders and to elucidate questions that relate to the idea of "maximally bonded" molecules.[69] However, the authors also point out that bond order is an interpretation, not an observable. In the present work, we developed an alternative interpretation of what is agreed on to constitute chemical reality, and our viewpoints do not contradict, but rather complement common views of chemical bonding.

In their perspective on the same subject, Weinhold and Landis remark that each generation of chemists readdresses and refines answers to questions of the nature of the chemical bond in the framework of its best current experimental and theoretical methods.[70] This statement is synonymous to a potential paradigm shift in chemical bonding, and the work by Bickelhaupt and Frenking—following ideas put forward in an earlier paper by Esterhuysen and Frenking[71]—is one of the first contributions that explicitly evaluate the importance of quasi-classical electrostatic interactions for what is regarded to be a covalent bond.[12] It is hoped that the present work supports the current efforts to refine and redefine chemical bonding.

Acknowledgements

KemKom expresses its gratitude to Professor L. Cavallo for granting access to the MoLNaC computing facilities at Dipartimento di Chimica, Università di Salerno, Italy.

[1] T. S. Kuhn, *The Structure of Scientific Revolutions*, University of Chicago Press, Chicago, **1962**.
[2] R. West, *ACS Symp. Ser.* **2005**, *917*, 166–178.
[3] J. Goubeau, *Angew. Chem.* **1957**, *69*, 77–82.
[4] P. Jutzi, *Angew. Chem.* **1975**, *87*, 269–283; *Angew. Chem. Int. Ed. Engl.* **1975**, *14*, 232–245.
[5] B. J. DeLeeuw, R. S. Grev, H. F. Schaefer, *J. Chem. Educ.* **1992**, *69*, 441–444.
[6] R. W. F. Bader, *Int. J. Quantum Chem.* **2003**, *94*, 173–177.
[7] a) G. Frenking, *Angew. Chem.* **2003**, *115*, 152–156; *Angew. Chem. Int. Ed.* **2003**, *42*, 143–147; b) R. J. Gillespie, P. L. A. Popelier, *Angew. Chem.* **2003**, *115*, 3452–3455; *Angew. Chem. Int. Ed.* **2003**, *42*, 3331–3334; c) G. Frenking, *Angew. Chem.* **2003**, *115*, 3456; *Angew. Chem. Int. Ed.* **2003**, *42*, 3335.
[8] P. W. Ayers, C. Morell, F. De Proft, P. Geerlings, *Chem. Eur. J.* **2007**, *13*, 8240–8247.
[9] a) C. A. Pignedoli, A. Curioni, W. Andreoni, *ChemPhysChem* **2005**, *6*, 1795–1799; b) G. Frenking, A. Krapp, S. Nagase, N. Takagi, A. Sekiguchi, *ChemPhysChem* **2006**, *7*, 799–800; c) C. A. Pignedoli, A. Curioni, W. Andreoni, *ChemPhysChem* **2006**, *7*, 801–802.
[10] F. M. Bickelhaupt, E. J. Baerends, *Rev. Comp. Ch.* **2000**, *15*, 1–86.
[11] R. S. Mulliken, *J. Am. Chem. Soc.* **1950**, *72*, 4493–4503.
[12] A. Krapp, F. M. Bickelhaupt, G. Frenking, *Chem. Eur. J.* **2006**, *12*, 9196–9216.
[13] R. S. Mulliken, *J. Am. Chem. Soc.* **1955**, *77*, 884–887.
[14] K. S. Pitzer, *J. Am. Chem. Soc.* **1948**, *70*, 2140–2145.
[15] R. West, M. J. Fink, J. Michl, *Science* **1981**, *214*, 1343–1344.
[16] H. Jacobsen, T. Ziegler, *J. Am. Chem. Soc.* **1994**, *116*, 3667–3679.
[17] G. Trinquier, J.-P. Malrieu, *J. Am. Chem. Soc.* **1987**, *109*, 5303–5315.
[18] E. A. Carter, W. A. Goddard, *J. Phys. Chem.* **1986**, *90*, 998–1001.
[19] H. Lischka, H. Köhler, *J. Am. Chem. Soc.* **1983**, *105*, 6646–6649.
[20] B. T. Colegrove, H. F. Schaefer, *J. Phys. Chem.* **1990**, *94*, 5593–5602.
[21] M. Bogey, H. Bolvin, C. Demuynck, J.-L. Destombes, *Phys. Rev. Lett.* **1991**, *66*, 413–416.
[22] M. Cordonnier, M. Bogey, C. Demuynck, J.-L. Destombes, *J. Chem. Phys.* **1992**, *97*, 7984–7989.
[23] K. Kobayashi, S. Nagase, *Organometallics* **1997**, *16*, 2489–2491.
[24] L. H. Pu, B. Twamley, P. P. Power, *J. Am. Chem. Soc.* **2000**, *122*, 3524–3525.
[25] A. D. Phillips, R. J. Wright, M. M. Olmstead, P. P. Power, *J. Am. Chem. Soc.* **2002**, *124*, 5930–5931.
[26] M. Stender, A. D. Phillips, R. J. Wright, P. P. Power, *Angew. Chem.* **2002**, *114*, 1863–1865; *Angew. Chem. Int. Ed.* **2002**, *41*, 1785–1787.
[27] A. Sekiguchi, R. Kinjo, M. Ichinohe, *Science* **2004**, *305*, 1755–1757.
[28] N. O. J. Malcolm, R. J. Gillespie, P. L. A. Popelier, *J. Chem. Soc. Dalton Trans.* **2002**, 3333–3341.
[29] P. P. Power, *Chem. Commun.* **2003**, 2091–2101.
[30] P. P. Power, *Organometallics* **2007**, *26*, 4362–4372.
[31] M. Lein, A. Krapp, G. Frenking, *J. Am. Chem. Soc.* **2005**, *127*, 6290–6299.
[32] J. C. Slater, *Phys. Rev.* **1951**, *81*, 385–390.
[33] S. H. Vosko, L. Wilk, M. Nusair, *Can. J. Phys.* **1980**, *58*, 1200–1211.
[34] a) J. P. Perdew, K. Burke, M. Ernzerhof, *Phys. Rev. Lett.* **1996**, *77*, 3865–3868; b) J. P. Perdew, K. Burke, M. Ernzerhof, *Phys. Rev. Lett.* **1997**, *78*, 1396.

 © 2010 Wiley-VCH Verlag GmbH & Co. KGaA, Weinheim

[35] a) G. te Velde, F. M. Bickelhaupt, S. J. A. van Gisbergen, C. Fonseca Guerra, E. J. Baerends, J. G. Snijders, T. Ziegler, *J. Comput. Chem.* **2001**, *22*, 931–967; b) C. Fonseca Guerra, J. G. Snijders, G. te Velde, E. J. Baerends, *Theor. Chem. Acc.* **1998**, *99*, 391–403; c) ADF 2006.01, SCM, Theoretical Chemistry, Vrije Universiteit, Amsterdam, http://www.scm.com.

[36] a) E. Van Lenthe, E. J. Baerends; J. G. Snijders, *J. Chem. Phys.* **1994**, *101*, 9783–9792; J. G. Snijders, *J. Chem. Phys.* **1993**, *99*, 4597–4610; J. G. Snijders, *J. Chem. Phys.* **1993**, *99*, 4597–4610; b) E. Van Lenthe, E. J. Baerends; J. G. Snijders, *J. Chem. Phys.* **1994**, *101*, 9783–9792.

[37] L. Versluis, T. Ziegler, *J. Chem. Phys.* **1988**, *88*, 322–328.

[38] E. Van Lenthe, A. Ehlers, E. J. Baerends, *J. Chem. Phys.* **1999**, *110*, 8943–8953.

[39] a) S. K. Wolff, *Int. J. Quantum Chem.* **2005**, *104*, 645–659; b) H. Jacobsen, A. Berces, D. P. Swerhone, T. Ziegler, *Comput. Phys. Commun.* **1997**, *100*, 263–276; c) A. Berces, R. M. Dickson, L. Y. Fan, H. Jacobsen, D. P. Swerhone, T. Ziegler, *Comput. Phys. Commun.* **1997**, *100*, 247–262; d) H. Jacobsen, A. Berces, D. P. Swerhone, T. Ziegler, *ACS Symp. Ser.* **1996**, *629*, 154–163.

[40] E. Van Lenthe, E. J. Baerends, *J. Comput. Chem.* **2003**, *24*, 1142–1156.

[41] E. J. Baerends, D. E. Ellis, P. Ros, *Chem. Phys.* **1973**, *2*, 41–51.

[42] Gaussian 03, Revision B05, M. J. Frisch, G. W. Trucks, H. B. Schlegel, G. E. Scuseria, M. A. Rob, J. R. Cheeseman, J. A. Montgomery, Jr., T. Vreven, K. N. Kudin, J. C. Burant, J. M. Millam, S. S. Iyengar, J. Tomasi, V. Barone, B. Mennucci, M. Cossi, G. Scalmani, N. Rega, G. A. Petersson, H. Nakatsuji, M. Hada, M. Ehara, K. Toyota, R. Fukuda, J. Hasegawa, M. Ishida, T. Nakajima, Y. Honda, O. Kitao, H. Nakai, M. Klene, X. Li, J. E. Knox, H. P. Hratchian, J. B. Cross, V. Bakken, C. Adamo, J. Jaramillo, R. Gomperts, R. E. Stratmann, O. Yazyev, A. J. Austin, R. Cammi, C. Pomelli, J. W. Ochterski, P. Y. Ayala, K. Morokuma, G. A. Voth, P. Salvador, J. J. Dannenberg, V. G. Zakrzewski, S. Dapprich, A. D. Daniels, M. C. Strain, O. Farkas, D. K. Malick, A. D. Rabuck, K. Raghavachari, J. B. Foresman, J. V. Ortiz, Q. Cui, A. G. Baboul, S. Clifford, J. Cioslowski, B. B. Stefanov, G. Liu, A. Liashenko, P. Piskorz, I. Komaromi, R. L. Martin, D. J. Fox, T. Keith, M. A. Al-Laham, C. Y. Peng, A. Nanayakkara, M. Challacombe, P. M. W. Gill, B. Johnson, W. Chen, M. W. Wong, C. Gonzalez, J. A. Pople, Gaussian, Inc., Wallingford CT, **2004**.

[43] A. Schäfer, H. Horn, R. Ahlrichs, *J. Chem. Phys.* **1992**, *97*, 2571–2577.

[44] N. Godbout, D. R. Salahub, J. Andzelm, E. Wimmer, *Can. J. Chem.* **1992**, *70*, 560–571.

[45] H. Stoll, *Chem. Phys. Lett.* **2006**, *429*, 289–293.

[46] W. Küchle, M. Dolg, H. Stoll, H. Preuss, *Mol. Phys.* **1991**, *74*, 1245–1263.

[47] P. L. A. Popelier, *Comput. Phys. Commun.* **1996**, *93*, 212–240.

[48] Jmol: an open-source Java viewer for chemical structures in 3D. http://www.jmol.org.

[49] T. Ziegler, *NATO ASI* **1992**, *C378*, 367–391.

[50] K. Kitaura, K. Morokuma, *Int. J. Quantum Chem.* **1976**, *10*, 325–340.

[51] T. Ziegler, A. Rauk, *Inorg. Chem.* **1979**, *18*, 1558–1565.

[52] K. Morokuma, *J. Chem. Phys.* **1971**, *55*, 1236–1244.

[53] H. Jacobsen, M. J. Fink, *Inorg. Chim. Acta* **2007**, *360*, 3511–3517.

[54] H. Jacobsen, A. Correa, A. Poater, C. Costabile, L. Cavallo, *Coord. Chem. Rev.* **2009**, *253*, 687–703.

[55] H. L. Schmider, A. D. Becke, *J. Mol. Struct.* **2000**, *527*, 51.

[56] H. L. Schmider, A. D. Becke, *J. Chem. Phys.* **2002**, *116*, 3184–3193.

[57] A. Savin, O. Jepsen, J. Flad, O. K. Andersen, H. Preuss, H. G. von Schnering, *Angew. Chem.* **1992**, *104*, 186–188; *Angew. Chem. Int. Ed. Engl.* **1992**, *31*, 187–188.

[58] R. F. W. Bader, *Atoms in Molecules: A Quantum Theory*, Oxford University Press, Oxford. **1990**.

[59] H. Jacobsen, *Can. J. Chem.* **2008**, *86*, 695–702.

[60] H. Jacobsen, *J. Comput. Chem.* **2009**, *30*, 1093–1102.

[61] W. Kutzelnigg, *Angew. Chem.* **1984**, *96*, 262–286; *Angew. Chem. Int. Ed. Engl.* **1984**, *23*, 272–295.

[62] H. Jacobsen, *Dalton Trans.* **2009**, 4252–4258.

[63] A. Sekiguchi, S. Z. Zigler, R. West, J. Michl, *J. Am. Chem. Soc.* **1986**, *108*, 4241–4242.

[64] B. S. Thies, R. S. Grev, H. F. Schaefer, *Chem. Phys. Lett.* **1987**, *140*, 355–361.

[65] B. T. Colegrove, H. F. Schaefer, *J. Am. Chem. Soc.* **1991**, *113*, 1557–1561.

[66] Y. Chen, M. Hartmann, M. Diedenhofen, G. Frenking, *Angew. Chem.* **2001**, *113*, 2107–2112; *Angew. Chem. Int. Ed.* **2001**, *40*, 2051–2055.

[67] S. Nagase, K. Kobayashi, N. Takagi, *J. Organomet. Chem.* **2000**, *611*, 264–271.

[68] K. Kobayashi, N. Takagi, S. Nagase, *Organometallics* **2001**, *20*, 234–236.

[69] C. R. Landis, F. Weinhold, *J. Am. Chem. Soc.* **2006**, *128*, 7335–7345.

[70] F. Weinhold. C. R. Landis, *Science* **2007**, *316*, 61–63.

[71] C. Esterhuysen, G. Frenking, *Theor. Chem. Acc.* **2004**, *111*, 381–389.

Received: September 6, 2009
Published online: November 24, 2009

 © 2010 Wiley-VCH Verlag GmbH & Co. KGaA, Weinheim